AJP

ISSN : 0971 - 3093

Vol 30, No 2, February, 2021

ASIAN JOURNAL OF PHYSICS

An International Peer Reviewed Research Journal

Advisory Editors : W. Kiefer & FTS Yu

(From left) W Kiefer, D P Tiwari and J P Mittal

ap

ANITA PUBLICATIONS

FF-43, 1st Floor, Mangal Bazar, Laxmi Nagar, Delhi-110 092, India

B O : 2, Pasha Court, Williamsville, New York-14221-1776, USA

Asian Journal of Physics
Vol. 30, No 2 (2021) 321-335
Available on: www.asianjournalofphysics.in

ap

Determination of accurate absolute Raman cross-sections of benzene and cyclohexane in the gas phase

Ankit Raj[1], Henryk A Witek[1,2], and Hiro-o Hamaguchi[1,2]

[1]*Department of Applied Chemistry and Institute of Molecular Science, National Chiao Tung University, Hsinchu 30010, Taiwan*

[2]*Center for Emergent Functional Matter Science, National Chiao Tung University, Hsinchu 30010, Taiwan*

Absolute Raman cross-section of a Raman transition governs the strength of its observed intensity. The knowledge of this property is crucial in understanding the nature of the Raman tensor and for direct quantitative applications of the Raman intensities. In this study, we determine the absolute differential Raman cross-sections of benzene and cyclohexane: two molecules of fundamental importance, used routinely in studies pertinent to Raman cross-sections. In our experiments, over 15 sets of pressure dependent Raman spectra were acquired on an intensity calibrated Raman spectrometer. The contribution of air, as an impurity, in the pressure readings was quantified. We used pure rotational Raman bands of molecular hydrogen, with known accurate Raman cross-sections as the intensity standards. The Raman cross-sections of the ring breathing mode in benzene (ν_2, 992.3 cm^{-1}) and cyclohexane (ν_5, 801.3 cm^{-1}) were determined in the gas phase, with uncertainty of 2.7 and 3.5%, respectively.

Keywords: Absolute Raman cross-section, Differential Raman cross-section, Raman intensities, Polarizability, Raman spectroscopy.

1 Introduction

Absolute Raman cross-section is a property of fundamental importance in quantitative Raman spectroscopy. From a basic standpoint, it gives the magnitude of the involved polarizability tensor invariants during the scattering process [1-3]. From the perspective of applications, it allows the observed Raman intensities to be used for direct quantitative analysis of the scattering species [4, 5].

Experimental determination of absolute Raman cross-sections has so far been performed using two broad strategies. The first approach is using the ratio of Rayleigh and Raman scattering cross-sections which are determined theoretically, followed by the subsequent measurement of either the Rayleigh or Raman intensities in an experiment. An analogous method involving the comparison of the total scattering intensity with the Raman intensities has also been used. Notable works employing these techniques include the report on the cross-sections of O_2, N_2 and CO_2 by Fenner *et al* [6] and Penney *et al* [7] and of H_2 and D_2 by Röhr [8]. Another approach is by comparing the observed Raman intensities to a reference whose Raman cross-section is already known with an acceptable level of accuracy. This method, based on the relative Raman intensities, has been widely employed due to its simplicity in the design of the experiment and the cancellation of errors arising from the experimental factors; the reference and the sample are measured on the same optical setup under identical geometry. Fouche and Chang [9,10], Colles and Griffiths [11], and recently Acosta-Maeda *et*

Corresponding author
e-mail: hwitek@mail.nctu.edu.tw (Henryk A Witek); *hhama@nctu.edu.tw* (Hiro-o Hamaguchi)

al [12] have used this approach for determining the Raman cross-sections of several organic molecules, using either benzene or cyclohexane as the reference. Novel techniques based on non-linear Raman spectroscopy have also been reported recently [13-15].

Benzene and cyclohexane are important references for the relative determination of absolute Raman cross-sections of other molecules. The Raman cross-sections of these two molecules have been carefully studied over time. Notable works on benzene were reported by Kato and Takuma [16] and Skinner and Nilsen [17], who compared the Raman scattering intensity to standard blackbody lamp while monitoring the laser intensity. Schomacker *et al* [18] determined the cross-section of liquid benzene by comparing the Raman scattering signal to the total scattering, and using the Raman to Rayleigh scattering intensity ratios. Udagawa *et al* [19] have reported the value for benzene determined using H_2 as the intensity reference while using theoretical value of polarizability anisotropy for H_2. Later Abe *et al* [20] have determined the Raman cross-sections of cyclohexane in the gas phase using the same methodology presented by Udagawa and co-workers, and subsequently used the obtained value of cyclohexane for a relative determination of Raman cross-section of other molecules including benzene. Raman cross-section of liquid cyclohexane have been reported by Colles and Griffiths [11] who used benzene-D6 as an internal standard in the relative determination approach. Trulson and Mathies [21] reported the values for both benzene and cyclohexane as liquids, by measurements on an integrating cavity calibrated using a D_2 lamp. Recently, Acosta-Maeda *et al* [12] reported the values for liquid cyclohexane determined by a comparison of the incident laser power and the scattered power measured on a standoff Raman instrument. These works have reported the values of Raman cross-sections with errors of 3 to 10%.

In the present work, we focus on the determination of the Raman cross-sections of these molecules in the gas phase with the aim to obtain updated values with higher accuracy from spectra acquired on our in-house accurately calibrated Raman spectrometer, and establish a starting point in our larger goal of tabulating the Raman cross-section of many more molecules. In our current approach, we determine the Raman cross-sections of the totally-symmetric ring breathing modes of benzene (992.3 cm^{-1}) and cyclohexane (801.2 cm^{-1}) utilizing the rotational Raman bands from molecular hydrogen ($\nu_{i=0}, J_{i=2} \rightarrow \nu_{f=0}, J_{f=4}$ at 814.0 cm^{-1} and $\nu_{i=0}, J_{i=3} \rightarrow \nu_{f=0}, J_{f=5}$ at 1034.2 cm^{-1}) as the reference. In preparation to the present study, we have calculated the matrix elements of the wavelength dependent polarizability tensor invariants, $\langle\psi_{v_i, J_i}|\Omega_\lambda|\psi_{(v_f, J_f)}\rangle$, where Ω_λ = mean polarizability, α or polarizability anisotropy, γ, for H_2, HD and D_2 with high accuracy (numerical uncertainty below 0.1%) [22]. This allows us to calculate the Raman cross-sections of specific rotation-vibration transitions in H_2, HD and D_2 with high accuracy, which are then used as reference in the procedure for the relative determination of Raman cross-sections. In this approach, the comparison of Raman intensities observed at different wavenumbers can introduce additional errors due to the variation in the wavenumber-dependent sensitivity of the Raman spectrometer. Hence, we performed an extensive intensity calibration of our spectrometer [23] utilizing relative intensities of the observed rotational Raman bands and the calculated matrix elements of polarizability, of H_2, HD and D_2. Accurate intensity calibration, with uncertainty of only 2% over a broad spectral range of over 2000 cm^{-1}, enables the analysis of Raman intensities from the reference (H_2) and our target molecules (benzene and cyclohexane) with minimal error, whose Raman bands are within 40 cm^{-1} of each other. The present approach of using H_2 as the reference for Raman cross-section is similar to the method adopted by Udagawa *et al* [19] and Abe *et al* [20] and improves on the technique by using updated and more accurate values of the wavelength dependent polarizability anisotropy, better instrumentation including real-time vapor pressure measurement and advancements in the data analysis.

In summary, the Raman cross-sections of totally-symmetric ring breathing vibration in benzene (992.3 cm^{-1}) and cyclohexane (801.3 cm^{-1}) were determined in the gas phase using rotational Raman bands from H_2 as the reference.

2 Experimental details

2.1 Method

Observed Raman intensity, I (photon counts) is given by [1,7]

$$I = \left(\frac{d\sigma}{d\Omega} \cdot P_i \cdot F_{laser} \cdot N \cdot \Omega \cdot D\right), \tag{1}$$

where $d\sigma/d\Omega$ is the differential Raman cross section (m^2molecule^{-1}steradian^{-1}), P_i is the Boltzmann population of the initial state for the specific Raman transition, F_{laser} is the luminance flux of incident laser (photon m^{-2} s^{-1}), N is the number of molecules in the focal volume, Ω is the observed solid angle (steradian), and D is the detection efficiency of the Raman spectrometer at the observed wavenumber position. Relative Raman intensity of the sample, s, to that of a reference, r, is then given as

$$\frac{I_s}{I_r} = \frac{\left(\frac{d\sigma_s}{d\Omega} \cdot P_{i,s} \cdot N_s \cdot D_s\right)}{\left(\frac{d\sigma_r}{d\Omega} \cdot P_{i,r} \cdot N_r \cdot D_r\right)}, \tag{2}$$

under the premise that, *i*) the sample and the reference are measured under identical conditions with the same laser power and exposure time, and ii) the focal volume is constant for both the sample and the reference. The difference in the detection efficiency over wavenumbers is corrected after the intensity calibration of the spectrometer, and under such condition the D_s and D_r terms in Eq (2) are dropped. Subsequently, Eq (2) is rearranged to obtain the absolute Raman cross-section of the sample $\frac{d\sigma_s}{d\Omega}$ to yield,

$$\frac{d\sigma_s}{d\Omega} = \frac{d\sigma_r}{d\Omega} \cdot \left(\frac{P_{i,r}}{P_{i,s}}\right) \cdot \left(\frac{I_s}{I_r}\right) \cdot \left(\frac{N_r}{N_s}\right) \tag{3}$$

In the current work, pure rotational Raman intensities from H_2 are used as the reference (I_r). The differential Raman cross-section of a pure rotational Stokes-Raman line ($\Delta J = +2$) from a diatomic molecule, for parallel polarized detection, is given by [1]

$$\frac{d\sigma}{d\Omega} = k_{\tilde{\nu}}\, \tilde{\nu}_o\, \tilde{\nu}_s^3 \left(\frac{2}{15}\right) \left(\frac{(J+1)(J+2)}{(2J+1)(2J+3)}\right) \left|\langle\gamma\rangle_{(v=0;\, J_i \rightarrow J_f)}\right|^2 \tag{4}$$

where $k_{\tilde{\nu}} = \pi^2/\epsilon_0^2$, $\tilde{\nu}_o\, \tilde{\nu}_s^3$ is the frequency factor composed of the absolute wavenumber of the excitation laser ($\tilde{\nu}_o$) and the scattered light ($\tilde{\nu}_s$), J is the initial rotational state of the specific transition and $\left|\langle\gamma\rangle_{(v=0;\, J_i \rightarrow J_f)}\right|^2 = \langle\psi_{v=0,\, J_i} \mid \gamma_\lambda \mid \psi_{v=0,\, J_f}\rangle^2$ is the square of the ro-vibrational matrix element of the wavelength dependent polarizability anisotropy for the particular transition defined by the initial (J_i) and the final (J_f) rotational states. Equation (4) is used to compute the differential Raman cross-section of the reference, $d\sigma_r/d\Omega$, required in the evaluation of Eq (3).

Details on the design of the present study and the involved approximations leading to the suitability of the above equations to this work are briefly discussed below. In the present work, Raman spectra from the sample and the reference are measured, using the same laser power on a rigid optical setup without altering the relative positions of the excitation laser and the sample chamber. Replacement of the sample is also performed with no disturbance to the sample chamber. The sample and the reference molecules are both investigated in the gas phase having similar refractive indices, leading to a negligible variation in the effective focal volumes. An elaborate intensity calibration procedure is performed for correcting the wavenumber dependent sensitivity change of the Raman spectrometer. This allows for the applicability of Eq (3) for the determination of the differential Raman cross-section of the sample.

The computation of the differential Raman cross-section of the reference (pure rotational Raman lines of H_2) using Eq (4) requires the square of ro-vibrational matrix elements of polarizability anisotropy, which we calculated in our previous work [22]. In the present experiment, we utilize the two pure rotational Raman bands from molecular hydrogen, $\nu_{i=0}, J_{i=2} \rightarrow \nu_{f=0}, J_{f=4}$ at 814.0 cm^{-1}, and $\nu_{i=0}, J_{i=3} \rightarrow \nu_{f=0}, J_{f=5}$ at 1034.2 cm^{-1}, which are close to the fully-symmetric ring breathing modes of cyclohexane (ν_5, 801.3 cm^{-1}) and benzene (ν_1, 992.3 cm^{-1}), respectively. Refer to Section S1 of the supplementary material for numerical values of the ro-vibrational matrix elements for these Raman transitions.

2.2 Raman spectrometer

A lab built confocal Raman micro-spectrometer based on the back-scattering geometry was used in the present experiments. The diagram of the optical setup is placed in Section S2 of the supplementary material. This instrument was described in detail in our previous reports [23,24]. In brief, the second harmonic of an actively stabilized CW Nd:YVO_4 laser (VerdiV5, Coherent) was used as the excitation source. The laser wavenumber was continuously monitored and stabilized to 18790.0125 (±0.009) cm^{-1}, using a high-resolution wavelength meter (WS-7, High Finesse). The power stability of this laser was examined earlier and the laser power was found to be stable within 2% over a period of 27 hours. The linearly polarized excitation laser beam was directed by a beam splitter (10R:90T) into an inverted microscope (iX71, Olympus), and was focused inside the sample chamber using a long working distance objective lens (20×, NA 0.25, f = 25 mm) with typical laser power of ~ 200 mW. Backscattered light passed through the beam splitter and was focused by a lens on a 100 μm pinhole, followed by another lens forming a collimated beam. Three volume Bragg-notch filters (OptiGrate) were used to remove the Rayleigh scattering. An analyzer (GTH10M-A, Thorlabs) mounted on a rotation mount was used to select the parallel polarized light for detection. An achromatic convex lens was used to focus the light on the polychromator slit (slit width = 120 μm). Light dispersed by the polychromator (f =50 cm, f/6.5, 600 g/mm; SP-2500i, Princeton Instruments) was detected by a thermoelectric cooled CCD (Andor Newton DU970N-BV operating at –85 °C). The CCD spectral window spanned 17129–19903 cm^{-1} (absolute) or from −1114 to +1660 cm^{-1} (relative to the laser).

2.3 Sampling setup

The sample chamber for gases was a lab designed custom built gas cell, consisting of an inner chamber made of quartz and outer jacket made of brass. This gas cell was mounted on a PTFE adaptor enabling a fixed placement on the microscope stage. The gas cell setup was connected to a vacuum manifold, consisting of two pumps and a liquid nitrogen trap, for removal of air and filling with gases for Raman measurements, and this process involved no physical disturbance to the gas cell. Absolute pressure of the gas was measured using a high-resolution pressure transducer (Omega PX409AUSBH, NIST calibrated) having uncertainty of 0.08% in a best-straight-line fit of several pressure readings over the range of the sensor. Additional details of the gas cell and the sampling setup are placed in Section S2 of the supplementary material.

2.4 Wavenumber and intensity calibration of the Raman spectrometer

Wavenumber calibration and intensity calibration was performed using the spectra of rotational Raman lines of H_2, HD, D_2 and O_2 gases, acquired prior to the main experiments on the differential Raman cross-sections. This calibration procedure was reported in full detail earlier [23] and only a brief description is given below.

Wavenumber calibration was done using the band positions of 45 pure rotational Raman lines from H_2, HD and D_2 (from 1034 to 1246 cm^{-1}) and 16 rotation-vibration Raman lines of O_2 (1400 to 1660 cm^{-1}). The accurate reference transition wavenumbers for these lines were obtained from previous experimental and theoretical works [25-27]. Errors in the wavenumber calibration was checked using emission lines from neon, and the 3σ uncertainty was ±0.3 cm^{-1}.

Accurate wavelength dependent polarizability anisotropy and ro-vibrational wavefunctions for H_2, HD and D_2 calculated by us previously were used to determine the rotational Raman intensities of these molecules. The Raman intensities were then effectively used as primary intensity calibration standards [23]. The relative experimental intensities for bands originating from common rotational states [28], and the corresponding accurate theoretical ratios were used with a non-linear least-squares fitting procedure to obtain the wavelength dependent sensitivity for intensity calibration. Temperatures determined using anti-Stokes to Stokes intensity ratios, from bands of carbon tetrachloride (218.1, 313.9 and 460.2 cm^{-1}), cyclohexane (801.3 cm^{-1}), and benzene (992.3 cm^{-1}) measured separately as liquids, were used to estimate the uncertainty of the sensitivity curve; which was found to be less than 2%, over the broad spectral range covering greater than 2000 cm^{-1}. (See Section S3 in the supplementary material for additional details on the intensity correction procedure.)

2.5 Raman measurements for differential Raman cross-sections

Raman spectra from the samples (benzene and cyclohexane in the gas phase) and the reference (H_2 gas) were acquired over an exposure time of 30 minutes, with the power of the excitation laser set to around 200 mW. Raman spectral acquisition was in synchronization with the pressure measurement using a controlling program written in LabVIEW [29,30]. Raman spectra from reference-sample pair were acquired on the same day to minimize the effect of laser power fluctuations on the observed Raman intensities.

H_2 (Chiah-Lung, Taiwan; 96% purity) was placed in the pre-evacuated gas cell and 16–22 spectra were acquired at several different pressures. Benzene (B0020, TCI Chemicals; > 99.5% purity) and cyclohexane (102822, Merck; 99.9% purity) were used without further purification. Approximately 25 mL of the liquid was placed in a thoroughly cleaned steel sample container and sealed using a valve. The dissolved gases from the liquid were removed by four cycles of *freeze-pump-thaw* procedure, followed by opening of the valve to the pre-evacuated gas cell. Temporal evolution of the pressure in the gas cell was followed by checking the readings from the pressure sensor. Raman measurements were started typically after 2 hours of opening of the valve, during which the vapor pressure value had reached to around 30–50 % of the saturated vapor pressure. It took another 3–5 hours for the vapor pressure to stabilize at around 90% of the saturated vapor pressure. Data on the temperature dependent vapor pressure [31] of benzene and cyclohexane are given in Section S4 of the supplementary material. A total of 16–22 spectra were measured for each of these two samples.

2.6 Data analysis

The following data analysis procedure was followed for all of the acquired spectra. First, the contribution from the quartz window was subtracted by a one-to-one subtraction of the spectra acquired from the evacuated gas cell. Second, intensity correction to the background subtracted spectra was performed using wavenumber dependent correction curves (determined earlier) for rectifying their relative Raman intensities. For details about the intensity calibration procedure, refer to Section 3.3 and Section S3 of the supplementary material. In the next step of data analysis, the area of the target band in the corrected Raman spectra was determined using band fitting. Single Gaussian function was used for fitting the 801.3 cm^{-1} band of cyclohexane. For the 992.3 cm^{-1} band of benzene, which has a smaller feature on the lower wavenumber side, two Gaussian functions were used, centered at 992.3 and 990.1 cm^{-1}. For both of the rotational Raman bands at 814 and 1034 cm^{-1} of H_2, a single Gaussian function was used for the fitting. Owing to the well-defined band shapes of the above mentioned Raman bands, the typical uncertainty in the band fitting procedure was below 0.6% as reported by the fitting program. The actual uncertainty was estimated as the square root of the band area plus an additional 1.25% of the band area which effectively covered any error encountered in the fitting procedure. Plots showing the measured Raman spectra of the gases at a fixed pressure are shown in Fig 1.

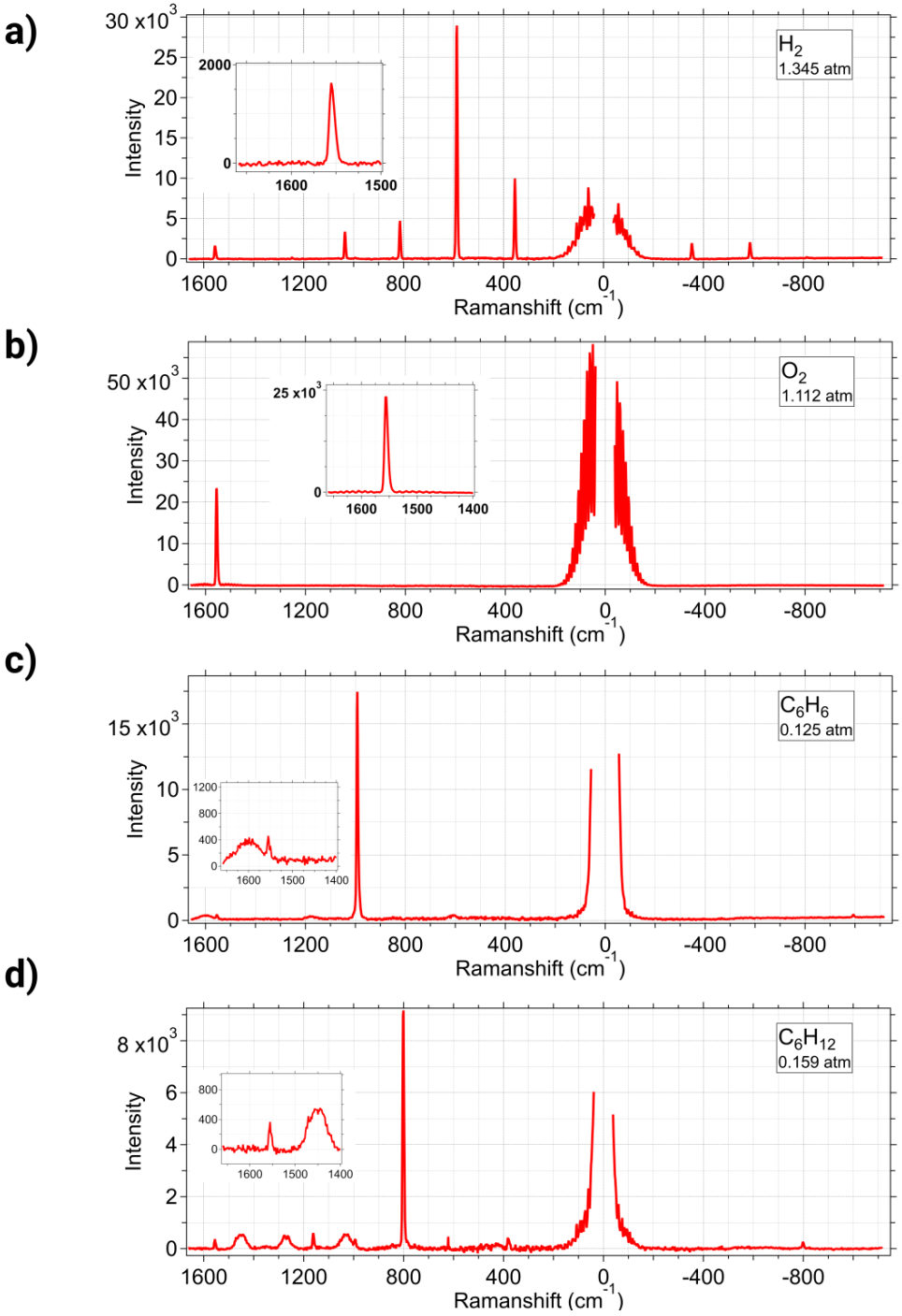

Fig 1. Raman spectra of gases, at the specified pressures, studied in this work. a) H_2 where the contamination from air is evident from the pure rotational Raman bands from N_2 and O_2 in the low wavenumber region and the vibration-rotation band of O_2 at 1556 cm^{-1}. b) high purity O_2, c) benzene, and d) cyclohexane. The fundamental band of O_2 at 1556 cm^{-1} is observed in all the plots.

Next, the time-dependent pressure readings recorded in synchronization with each of the Raman spectra were analyzed. Since the observed Raman intensity is temporally averaged over the duration of the exposure time (30 minutes in the present experiments), mean of the pressure data was computed, having an estimated uncertainty of 1%, and these were used for further analysis. This is justified since the observed Raman intensity is linearly proportional to the number of molecules, which is equivalent to the pressure for gases.

In the next step, sets of Raman spectra from benzene, cyclohexane and H_2 were examined to identify minor features from impurities, and spectral signatures from O_2 and N_2 (from air) were found in this assessment. Since the total pressure was recorded during the experiments, further analysis was undertaken to quantify the partial pressures of these impurities to obtain the actual pressure of the samples and the reference. This analysis is discussed in the following section.

2.7 Quantifying the contamination from air as an impurity

During the Raman measurement of gaseous benzene and cyclohexane, the gas cell was kept at low pressures over a considerable period of time. Contamination from air in the gas cell was expected in this time interval, due to, imperfect sealing of the gas setup, slow degassing from the O-rings and/or transfer of any residual dissolved gases from the liquid, to the partial vacuum inside the gas cell. Hence, we expected the presence of Raman signals from N_2 and O_2, the two major constituents of air, in the acquired Raman spectra. The measured Raman spectra of the samples showed minute spectral intensity for the fundamental vibration from O_2 observed at 1556 cm^{-1}. The pure rotational Raman features from both N_2 and O_2 were obscured in the Raman spectra of benzene and cyclohexane due to the Rayleigh wings, while the fundamental band of N_2 at 2330 cm^{-1} was outside our spectral region of investigation.

In the case of H_2, our gas supply was only 96% pure, with the impurity stated to be air. The Raman spectra of H_2 showed spectral signatures from both O_2 (fundamental at 1556 cm^{-1}) and the pure rotational Raman features from both O_2 and N_2 below 150 cm^{-1}.

The pressure sensor used in the current experiments reported the total absolute pressure. The contribution of the pressure from O_2 and N_2 as the primary impurities, existent in the measured total pressure was thus required to be estimated. For this purpose, we measured a total of 30 Raman spectra of O_2 (Chiah-Lung, Taiwan; > 99% purity) at several different pressures. The pressure dependent Raman intensity profile for O_2 was established (as a linear function), using the band area of the fundamental band from the set of O_2 spectra (shown later in Section 4). The band area was determined by fitting the band using two Gaussian functions. The partial pressure of O_2 during the measurement of benzene, cyclohexane and H_2 was then estimated using the observed Raman intensities in their respective spectra and the determined intensity-to-pressure relationship. The partial pressure of air, P_{air}, was estimated using the mole fraction of O_2 in standard air [32] (0.20946 mol%) as (1/0.20946) $P_{O_2} = 4.77418 \times P_{O_2}$; while assuming that air is the major component of the possible impurities. The contributions from other possible minor components, such as the isotopic fractions of N_2 and O_2 and any volatile components in the benzene and cyclohexane, were not considered. Having found the partial pressure of air as impurity from the intensity of the band from O_2, the actual pressure of the sample or reference was then determined for each of their measured spectra as : Total pressure – P_{air}.

3 Results

Intensity of the fundamental band of O_2 was used to determine the partial pressure of air, present as impurity during the Raman measurement of the reference and the samples. In this process, the Raman intensity-dependent-pressure relationship was first established using 30 Raman spectra of pure O_2 measured at different pressures. Figure 2 shows the measured pressure of O_2 plotted against the measured Raman intensity of the fundamental band. Linear fit of these data points yielded the relationship, $P_{O_2} = (0.57921 \times I_{O_2})$.

Thereafter, using this relationship and the intensity of the O_2's band in the Raman spectra of samples and reference, the partial pressure of O_2 was determined. Subsequently the partial pressure of air, P_{air}, as impurity was found (for more details see Section 3.6). The magnitude of P_{air} relative to the total pressure reading was 3.8–5.8% in the case of H_2, 10–50% in the case for benzene and 10–75% in the case of cyclohexane. This exemplifies the importance of the examination of the impurities during the Raman measurements of gases and devising proper corrections to the recorded pressure value. Actual pressures of the benzene, cyclohexane and H_2 were then determined by subtracting the contribution of P_{air} from the total pressure. Appropriate proportion of error in final pressure value originating due to the above data treatment, was taken into account during the further analysis.

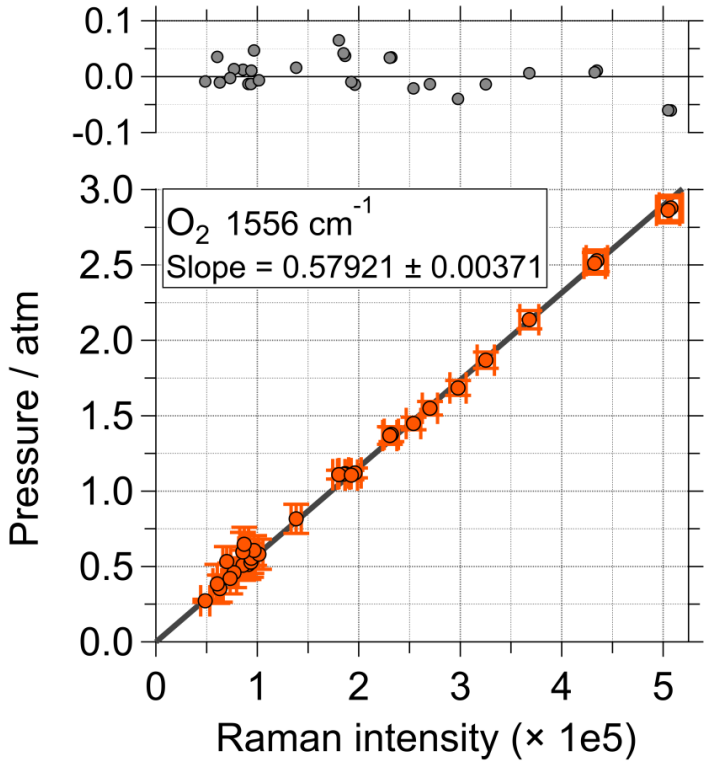

Fig 2 . Results obtained from the pressure dependent Raman measurements of O_2, to determine the relationship of Raman intensity to the pressure of the gas, on our Raman spectrometer. The measured pressures of O_2 is plotted against the recorded Raman band areas of the fundamental band of O_2 observed at 1556 cm^{-1}. The slope of the linear fit (shown in grey line) was used for intensity-to-pressure conversion in our analysis (see Section 3.6).

Band areas of the pure rotational Raman transition ($v_{i=0}, J_{i=3} \rightarrow v_{f=0}, J_{f=5}$) observed at 1034 cm^{-1} from H_2, from 21 spectra acquired at varying pressures are shown in Fig 3 (a). Corresponding data, from 22 measurements, for the ring breathing mode of gaseous benzene at 992.3 cm^{-1}, measured after H_2 with same laser power and exposure time, is shown in Fig 3 (b). Similar plots for the 814 cm^{-1} ($v_{i=0}, J_{i=2} \rightarrow v_{f=0}, J_{f=4}$) transition of H_2, and 801.3 cm^{-1} band of cyclohexane, as the reference-sample pair, are shown in Figs 4 (a) and 4 (b), respectively. Here, both the reference and the sample have 16 data points each.

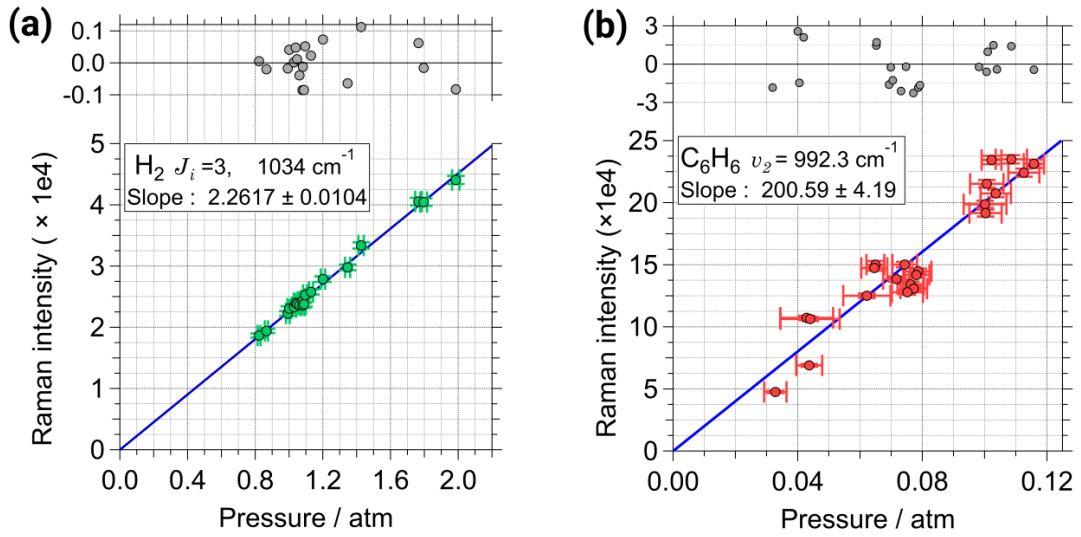

Fig 3. Experimental pressure dependent Raman intensity data from; a) the 1034 cm^{-1} band of H_2 as the reference, shown in green color; and b) the 992.3 cm^{-1} band of gaseous benzene as the sample, for Raman cross-section determination, shown in red color. For both the reference and the sample, the slopes are determined from a least-squares linear fit of the data, with the intercept fixed to zero. Uncertainties in both x- and y-directions are considered in the fit and the 1σ errors in the slopes are mentioned. Residuals are shown on top in grey color.

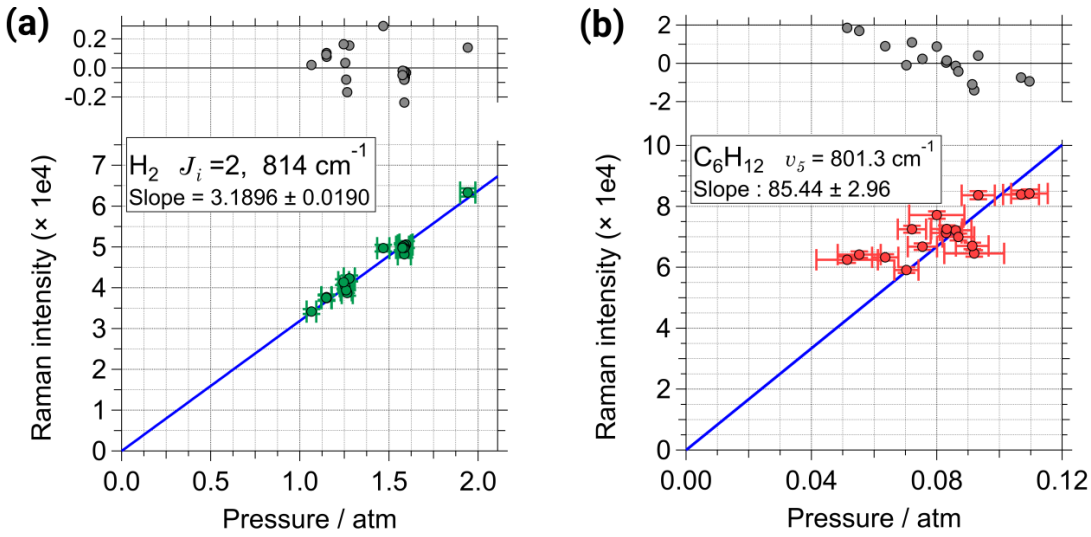

Fig 4. Experimental pressure dependent Raman intensity data from; a) the 814 cm^{-1} band of H2 as the reference, shown in green color; and b) the 801.3 cm^{-1} band of gaseous cyclohexane as the sample, for the Raman cross-section determination, shown in red color. For both the reference and the sample, the slopes are determined from a least-squares linear fit of the data, with the intercept fixed to zero. The 1σ error in the values of the slopes are noted. Residuals are shown on top in grey color.

Table 1. Differential Raman cross-sections, $(d\sigma/d\Omega) \times 10^{-30}$ cm^2 sr^{-1} molecule^{-1} , of gaseous benzene and cyclohexane, at 532.2 nm. Interpolated values from previous works are listed for a comparison. Results acquired at using other wavelength excitation were interpolated using the frequency factor to the present wavelength. Results from liquid measurements were converted to approximate values in the gas phase using the local field correction.

Benzene (gaseous)			
Present work	**Previous works**		**Phase**
6.052 (±0.163, 2.7%, 1σ)	Ref. 19[a]	6.56 (±0.33, 5%)	Gas
	Ref. 20[b]	6.56 (±0.33, 5%)	Gas
	Ref. 2[c]	4.95 (±0.48, 9.8%)	Gas
	Ref. 6[d]	2.09 (±0.69, 33%)	Gas
	Ref. 16[e]	5.56 (±0.17, 3%)	Liquid
	Ref. 21[f]	7.77 (±0.51, 6.6%)	Liquid
	Ref. 17[g]	1.78 (±0.14, 7.6%)	Liquid
	Ref. 18[h]	6.43 (±0.63, 9.8%)	Liquid
Cyclohexane (gaseous)			
Present work	**Previous works**		**Phase**
2.501 (±0.087, 3.5%, 1σ)	Ref. 20[b]	2.18 (±0.12, 4.7%)	Gas
	Ref. 21[f]	2.18 (±0.10, 4.6%)	Liquid
	Ref. 11[i]	2.33 (±0.23, 10%)	Liquid
	Ref. 12[j]	1.476	Liquid

a: λ_{exc} = 514.5 nm. Using pure rotational Raman band of H_2 at 1034 cm^{-1} as the reference.

b: λ_{exc} = 514.5 nm. Using pure rotational Raman band of H_2 at 1034 cm^{-1} as the reference.

c: λ_{exc} = 488 nm. Using fundamental of N_2 at 2330 cm^{-1} as the reference.

d: λ_{exc} = 488 nm. Using fundamental of N_2 at 2330 cm^{-1} as the reference.

e: λ_{exc} = 488 nm. Blackbody radiator furnace as the radiation standard.

f: λ_{exc} = 647, 514.5, 476, 407 and 351 nm. Direct measurement of the incident laser power and scattered intensity using an integrating cavity.

g: λ_{exc} = 488 nm. Direct measurement of the incident laser power and scattered intensity on a setup with known efficiency of optical components.

h: λ_{exc} = 514.5, 488, 441.6 and 325 nm. Interpolated value using data at 514.5 nm.

i: λ_{exc} = 488 nm. C_6D_6 as the internal standard.

j: λ_{exc} = 532 nm. Direct measurement of the scattered power and incident laser power. Error not mentioned.

The slope of the Raman intensity-vs-pressure curve correspond to the observed intensity divided by the number of molecules, I/N , required during the solution of Eq (3), when determining the Raman cross-section of the sample. Therefore, the slope for the reference, $m_r = I_r/N_r$, obtained from the experimental data on H_2 (in Figs 3 (a) and 4 (a)) and the slope for the target samples, $m_s = I_s/N_s$, obtained from the experimental data on benzene or cyclohexane (in Figs 3 (b) and 4 (b)) were used in our analysis. Boltzmann populations at the measured temperatures, for the initial states of the specific transitions studied in the samples and reference were computed. These along with the absolute Raman cross-section(s) of the reference bands, were used to determine the absolute Raman cross-section of the samples. The obtained results

were, 6.052 (1σ = 0.163, 2.7%) and 2.501 (1σ = 0.087, 3.5%), expressed as 10^{-30} cm^2 sr^{-1} molecule^{-1}, for benzene and cyclohexane, respectively. These results are for Raman scattered photons having polarization parallel to the incident laser ($\|_{detetection}$,$\|_{incident}$), and the known depolarization ratios [2] of the studied Raman bands allow for a straightforward determination of corresponding values for the detection of both the polarizations ($\| + \perp_{detetection}$, $\|_{incident}$). Present numbers together with the results from previous works are listed in Table 1. Results from literature were interpolated to the present excitation wavelength using the frequency factor ($\nu_o\ \nu_s^3$) if the excitation wavelength was different from the present work. The results on liquid samples were converted to approximate values in the gas phase using the local-field correction [20,33,34], $\left(\frac{d\sigma}{d\Omega}\right)_{gas} = L^{-1}\left(\frac{d\sigma}{d\Omega}\right)_{liq}$, where, $L = \left(\frac{n_s}{81 n_0}\right)(n_s^2 + 2)^2\ (n_0^2 + 2)^2$, and n_s and n_o are the wavelength dependent refractive indices of the liquid at the scattered and the incident wavelengths, respectively.

3.1 Error estimation

The net error in the absolute differential Raman cross-section of the sample was determined using standard expression for error propagation, derived for Eq (3), where the I/N terms were replaced with the slope determined from the experimental data. The equation used is given below:

$$\Delta\left(\frac{d\sigma_s}{d\Omega}\right) = \left(\frac{d\sigma_s}{d\Omega}\right) \times \sqrt{\left(\frac{\Delta m_s}{m_s}\right)^2 + \left(\frac{\Delta m_r}{m_r}\right)^2 + \left(\frac{\Delta(d\sigma_r/d\Omega)}{d\sigma_r/d\Omega}\right)^2} \tag{5}$$

Here, $(d\sigma_s/d\Omega)$ is the obtained value of the Raman cross-section of the sample, Δm_s and Δm_r are the uncertainties in the slopes (m_s and m_r) of the sample and the reference, respectively, determined from sets of experimental data, and lastly $\Delta\,(d\sigma_r)/d\Omega$ is the uncertainty in the value of the Raman cross-section of the reference, $d\sigma_r\,/d\Omega$.

In the error estimation process, we used 1σ standard deviation in the slopes determined during the least squares fit, as Δm_s and Δm_r, while $\Delta\,(d\sigma_r/d\Omega)$ was estimated from the uncertainty in the numerical value of matrix element of polarizability anisotropy, required in the computation of the Raman cross-section of the reference (see Eq (4) and Section S1 of the supplementary material for more details). The magnitudes of uncertainties in the individual sources of error was, typically 2–3% for the slopes of the samples, below 1% for both the slope(s) of the reference and below 0.5% for the Raman cross-section of the reference. Additional error of 0.5% for benzene and 0.1% for cyclohexane was included to account for the purity of these samples. The net error (1σ) in the determined absolute (differential) Raman cross-section was 2.7 % for benzene and 3.5% for cyclohexane.

4 Discussion

In the following discussion, the values of the differential Raman cross-sections have the unit: (dσ/dΩ) ×10^{-30}) cm^2 sr^{-1} molecule^{-1}, and only the leading significant digits are mentioned for clarity.

Table 1 shows that overall, the present results are in good correspondence with the previous reports. It is, however, observed that literature values are spread over a large range. For benzene, our value (**6.052**, **± 0.163**) is in between the results by Abe *et al* [20] (6.56, ± 0.33) obtained using H_2 as the reference, and by Fernández-Sánchez and Montero [2] (4.95, ± 0.48) who used the intensity of the fundamental of N_2 at 2330 cm^{-1}, as the intensity reference. Value reported by Fenner *et al* [6] (2.09, ±0.69), also determined relative to N_2, is substantially away from the present result and also from other gas phase values. Results obtained from liquid benzene are compared next, which have been converted to analogous gas phase values. Present result is in agreement with the number reported by Schomacker

et al [18] (6.43, ± 0.63), determined by a measurement of the incident and the scattered light. Whereas, our value is in disagreement with the analogous values (1.78, ± 0.14) by Skinner and Nilson [17] and by Trulson and Mathies [21] (7.77, ± 0.51), both obtained by measurement of incident and scattered power, but with different optical setups. Our results are greater than the value obtained for liquid benzene by Kato and Takuma [16] (5.56, ± 0.17), who measured the scattered power against radiation from a black-body furnace while noting the incident laser. It is worthwhile to mention that results by Fenner *et al* on gas phase benzene (2.09, ±0.69) and by Skinner and Nilson determined for liquid benzene (1.78, ± 0.14), are close.

Results on the absolute Raman cross-section of gaseous cyclohexane are rather limited. The present value for cyclohexane (**2.501, ± 0.087**) is greater than the numbers reported by Abe *et al* (2.18, ± 0.12) for gaseous samples and by Trulson and Mathies [21] for liquid sample (2.18, ±0.10). Present value it is closer to the value by Colles and Griffiths [11] (2.33, ± 0.23) whose results have a larger error, determined relative to the 944 cm^{-1} band of benzene-D6, as the internal reference. Our gas phase result is significantly away, from the value for liquid cyclohexane, recently reported by Acosta-Maeda *et al* [12] (1.476). Notably, results by Abe *et al* and Trulson and Mathies are in good agreement with each other, for cyclohexane but not for benzene.

Results from Udagawa *et al* [19] and Abe *et al* [20] (from the same research group) do require further mention. Their values were determined using rotational Raman lines from H_2 as an intensity reference, similar to this study. For benzene, the present results are smaller than their results, 6.052 (our) vs 6.56 (Ref 20), while for cyclohexane, the present values are larger, 2.501 (our) vs 2.18 (Ref 20). General scheme of the experiment in the work of Udagawa *et al* and Abe *et al* is same as the present study, where a mercury manometer was used to measure the vapor pressure. However, details on the impurities in the measured samples and the accuracy of pressure measurement are lacking in their work. This makes it difficult to identify the source of discrepancy between the present values and those reported in Refs 19 and 20, as well as other previous works; only more experiments can possibly clarify the situation.

The present experiments employed *state-of- the-art* instrumentation with accurate pressure measurements evident in the linear trend of the Raman intensity-vs-pressure plots shown for the gases (Figs 1, 2 and 3). We identified air as an impurity existing in the sample chamber during the Raman measurements and devised corrections to the recorded total pressure values using the spectral signature of O_2. The experiments were complemented with the highly accurate values of the absolute Raman cross-sections of the reference (H_2), for which the calculations for wavelength dependent polarizability anisotropy were done earlier. The utilization of multiple data points (16 or more pairs) of pressure dependent Raman intensity values, was a major factor lowering the error introduced due to the prominent distribution of vapor pressure in the case of benzene and cyclohexane. Furthermore, this enhanced the reliability of our data analysis by reducing the impact of outlying values. These overall advancements lead to a considerable reduction in the uncertainties of the present results, noticeable in Table 1.

Nonetheless, there is significant room for improvement, particularly in the experimental techniques of the present study. One large contribution of error is from the contamination of the sample chamber with air. This causes substantial spread in the pressure values (and increase in the uncertainties) especially for gaseous benzene and cyclohexane, whose vapor pressures are relatively low at room temperatures (< 0.14 atm at 298 K) [31]. Condensation from the vapor phase benzene and cyclohexane on the walls of the gas setup (also noted by Fernández-Sánchez and Montero [2]), results in a longer duration for gas-liquid equilibrium to be established, and using a smaller sized gas-setup should help. Temporal variation in the laser power leads to fluctuations in the observed Raman intensities, which is another source of error. This can be significant, up to 2%, for present experiments since the spectra from the reference and sample are acquired at different times with a gap of several hours. Compensation for the deviation in laser power determined by a real-time laser power measurement will be required to minimize this error.

5 Conclusions

The absolute differential Raman cross-section of the totally symmetric ring breathing mode in gaseous benzene (ν_2, 992.3 cm^{-1}) and cyclohexane (ν_5, 801.3 cm^{-1}), were determined using 532.2 nm laser. The Raman cross-sections were obtained by comparison of the observed Raman intensities from these molecules with the intensities of the pure rotational Raman bands of H_2 (at 1034 and 814 cm^{-1}) as the reference, whose absolute Raman cross-sections were calculated with high accuracy.

The Raman cross-sections of benzene and cyclohexane have been frequently used for a relative determination of the Raman cross-sections of other molecules.[11,35,36]. Hence, the present results, with improved accuracy are particularly important for future experiments on this subject. With regard to the studies on the vibrations of benzene and cyclohexane, the reported values are required for obtaining accurate value of effective Raman tensor components for the studied vibrational modes [2]. Present experimental values for the gas phase, may be used as a standard for comparing analogous results from ab-initio calculations, typically performed for molecule(s) in vacuum.

The present technique of employing large dataset on the pressure (or concentration) dependent Raman spectra, for the relative determination of Raman cross-sections is shown to be a powerful approach. This method is easily extensible to other molecules of interest, both in the gas and liquid phase for such studies.

Supplementary material and data availability

Supplementary Material (6 pages) includes the following content. Sec. S1: Details on the computation of Raman cross-section(s), with tabulation of the ro-vibrational matrix elements for H_2 and the computed Boltzmann populations. Sec. S2: Additional details on the experimental setup (diagram of the Raman spectrometer and the sampling setup); Sec. S3: Intensity calibration of the Raman spectrometer; and Sec. S4: Temperature dependent vapor pressure data for benzene and cyclohexane.

Acknowledgements

This work was supported by Ministry of Science and Technology of Taiwan (Grant Nos. MOST105-2923-M-009-001-MY3, MOST108-2113-M-009-010-MY3, MOST103-2113-M-009-001 and MOST110-2923-M-009-004-MY3) and the Center for Emergent Functional Matter Science of National Chiao Tung University from the Featured Areas Research Center Program within the framework of the Higher Education Sprout Project by the Ministry of Education (MOE), Taiwan.

References

1. Long D A The Raman Effect : A Unified Treatment of the Theory of Raman Scattering by Molecules, (New York: Wiley), 2003.
2. Fernández-Sánchez J M, Montero S, Gas-Phase Raman-Scattering Cross-Sections of Benzene and Perdeuterated Benzene, *J Chem Phys*, 90(1989)2909-2914.
3. Avila G, Tejeda G, Fernandez J M, Montero S, The rotational Raman spectra and cross sections of H_2O, D_2O, and HDO, *J Mol Spectrosc*, 220(2003)259-275.
4. Pelletier M J, Quantitative Analysis Using Raman Spectrometry, *Appl Spectrosc*. 57(2003)20A-42A.
5. McCreery R L Raman spectroscopy for chemical analysis, (New York: J Wiley), 2000.
6. Fenner W R, Hyatt H A, Kellam J M, Porto S P S, Raman cross section of some simple gases, *J Opt Soc Am*, 63(1973)73-77.
7. Penney C M, St Peters R L, Lapp M, Absolute rotational Raman cross sections for N_2, O_2, and CO_2, J Opt Soc Am, 64(1974)712-716.

8. Röhr H, Rotational raman-scattering of hydrogen and deuterium for calibrating thomson scattering devices, *Phys Lett A*. 81(1981)451-453.
9. Fouche D G, Chang R K, Relative Raman Cross Section for O_3, CH_4, C_3H_8, NO, N_2O, and H_2, *Appl Phys Lett*, 20(1972)256-257.
10. Fouche D G, Chang R K, Relative Raman Cross Section for N_2, O_2, C_O, CO_2, SO_2, and H_2S, *Appl Phys Lett*, 18(1971)579-580.
11. Colles M J, Griffiths J E, Relative and Absolute Raman Scattering Cross Sections in Liquids, *J Chem Phys*, 56(1972)3384-3391.
12. Acosta-Maeda T E, Misra A K, Porter J N, Bates D E, Sharma S K, Remote Raman Efficiencies and Cross-Sections of Organic and Inorganic Chemicals, *Appl Spectrosc*, 71(2017)1025-1038.
13. Silva W R, Keller E L, Frontiera R R, Determination of Resonance Raman Cross-Sections for Use in Biological SERS Sensing with Femtosecond Stimulated Raman Spectroscopy, *Anal Chem*, 86(2014)7782-7787.
14. McAnally M O, Phelan B T, Young R M, Wasielewski M R, Schatz G C, Van Duyne R P, Quantitative Determination of the Differential Raman Scattering Cross Sections of Glucose by Femtosecond Stimulated Raman Scattering, *Anal Chem*, 89(2017)6931-6935.
15. Burns K H, Srivastava P, Elles C G, Absolute Cross Sections of Liquids from Broadband Stimulated Raman Scattering with Femtosecond and Picosecond Pulses, *Anal Chem*, 92(2020)10686-10692.
16. Kato Y, Takuma H, Absolute Measurement of Raman-Scattering Cross Sections of Liquids, *J Opt Soc Am*, 61(1971)347-350.
17. Skinner J G, Nilsen W G, Absolute Raman Scattering Cross-Section Measurement of the 992 cm^{-1} Line of Benzene*, *Anal Chem*, 58(1968)113-119.
18. Schomacker K T, Delaney J K, Champion P M, Measurements of the Absolute Raman Cross-Sections of Benzene, *J Chem Phys*, 85(1986)4240-4247.
19. Udagawa Y, Mikami N, Kaya K, Ito M, Absolute intensity ratios of Raman lines of benzene and ethylene derivatives with 5145 Å and 3371 Å excitation, *J Raman Spectrosc*, 1(1973)341-346.
20. Abe N, Wakayama M, Ito M, Absolute Raman intensities of liquids, *J Raman Spectrosc*, 6(1977)38-41.
21. Trulson M O, Mathies R A, Raman Cross-Section Measurements in the Visible and Ultraviolet Using an Integrating Cavity - Application to Benzene, Cyclohexane, and Cacodylate, *J Chem Phys*, 84(1986)2068-2074.
22. Raj A, Hamaguchi H, Witek H A, Polarizability tensor invariants of H_2, HD, and D_2, *J Chem Phys*. 148(2018)104308; doi.org/10.1063/1.5011433
23. Raj A, Kato C, Witek H A, Hamaguchi H, Toward standardization of Raman spectroscopy: Accurate wavenumber and intensity calibration using rotational Raman spectra of H_2, HD, D_2, and vibration–rotation spectrum of O_2, J Raman Spectrosc. 51(2020)2066-2082.
24. Raj A, Witek H A, Hamaguchi H, Vibration–rotation interactions in H_2, HD and D_2 : centrifugal distortion factors and the derivatives of polarisability invariants, *Mol Phys*. 118(2020)e1632950; doi.org/10.1080/00268976.2019.1632950.
25. Komasa J, Piszczatowski K, Łach G, Przybytek M, Jeziorski B, Pachucki K, Quantum Electrodynamics Effects in Rovibrational Spectra of Molecular Hydrogen, *J Chem Theory Comput*, 7(2011)3105-3115.
26. Pachucki K, Komasa J, Rovibrational levels of H D, *Phys Chem Chem Phys*, 12(2010)9188-9196.
27. Edwards H G M, Long D A, Najm K A B, Thomsen M, The vibration-rotation Raman spectra of $^{18}O_2$, $^{17}O^{18}O$, $^{17}O_2$ and $^{16}O_2$, *J Raman Spectrosc*, 10(1981)60-63.
28. Okajima H, Hamaguchi H, Accurate intensity calibration for low wavenumber (–150 to 150 cm^{-1}) Raman spectroscopy using the pure rotational spectrum of N_2, *J Raman Spectrosc*, 46(2015)1140-1144.
29. Kirkman I W, Buksh P A, Data acquisition and control using National Instruments' ''LabVIEW'' software, *Rev Sci Instrum*, 63(1992)869-872.
30. Kalkman C J, LabVIEW: A software system for data acquisition, data analysis, and instrument control, *J Clin Monit Comput*, 11(1995)51-58.

31. Onken U, Rarey-Nies J, Gmehling J, The Dortmund Data Bank: A computerized system for retrieval, correlation, and prediction of thermodynamic properties of mixtures, *Int J Thermophys*, 10(1989)739-747.
32. Warneck P, Wurzinger C, Chapter 10, Physical and Chemical Properties of the Air, (ed) Fischer G, (Berlin/ Heidelberg: Springer-Verlag), 1988.
33. Nestor J R, Lippincott E R, The effect of the internal field on Raman scattering cross sections, *J Raman Spectrosc*, 1(1973)305-318.
34. Eckhardt G, Wagner W G, On the calculation of absolute Raman scattering cross sections from Raman scattering coefficients, *J Mol Spectrosc*, 19(1966)407-411.
35. Acosta-Maeda T E, Misra A K, Muzangwa L G, Berlanga G, Muchow D, Porter J, Sharma S K, Remote Raman measurements of minerals, organics, and inorganics at 430 m range, *Appl Opt*, 55(2016)10283-10289.
36. Carlson R W, Fenner W R, Absolute Raman Scattering Cross-Section of Molecular Hydrogen, *Astrophys J* 178(1972)551-556.

[*Received*: 20.01.2021: *accepted*: 01.02.2021]

Ankit Raj is a doctoral student working with Prof. H Hamaguchi and Prof. H Witek on the broad goal of standardization of Raman spectroscopy and the determination of Raman cross-sections. Accurate measurements of Raman intensities and their applications are focus of his research.

Henryk A. Witek is a mathematically-oriented chemist of Polish origin living and working in Taiwan. He currently works as a professor of chemistry in the National Chiao Tung University (NCTU) in Hsinchu. He obtained his scientific degrees from the Jagiellonian University (MS) and from the University of Tokyo (PhD). His scientific research in the last few years is focused on exactly solvable models of quantum mechanics with particular emphasis on the analytical exact solution of the Schrödinger equation for the helium atom.

Hiro-o Hamaguchi received his D. Sc. Degree in physical chemistry from the University of Tokyo in 1975. In 1990, he became a laboratory head at the Kanagawa Academy of Science and Technology. From 1997 till 2012, he was a Professor of Chemistry at the University of Tokyo. He is now a Life Chair Professor at Department of Applied Chemistry, National Chiao Tung University, Taiwan. His recent research efforts are directed toward the elucidation of complex molecular systems including solutions and liquids, ionic liquids, and also living cells and human organs, using time- and space-resolved vibrational spectroscopy. He is the author of 296 scientific papers in the field of physical chemistry and molecular spectroscopy. His professional services include associate editors/editorial advisory members of eight international journals, chairs of five international conferences, President of the Spectroscopical Society of Japan and

President of the Japan Society of Medical Spectroscopy. He received Meggers Award (2005), the Spectroscopical Society of Japan Award (2006), Chemical Society of Japan Award (2009), TRVS Award (2009), Medal with purple ribbon from the Emperor of Japan (2012) and most recently, The order of the sacred treasure, gold rays with neck ribbon from the Emperor of Japan (2020). He was a Carl Zeiss Visiting Professor (2013) and a Mizushima-Raman Lecturer (2014). He is a Fellow of the Society of Applied Spectroscopy. His hobby is watching nature, in particular, collecting Taiwanese stag beetles.